Supplementary Material (ESI) for Soft Matter: **Mechanical properties of mushroom and brush poly(ethylene glycol)-phospholipid membranes**†

Stefan Kaufmann,[a] **Oleg Borisov,**[b], **Marcus Textor,**[a] **and Erik Reimhult**[*c]

DOI: 10.1039/b000000x

1 Formation of PEG-SLBs with 4 - 10 mol% DOPE-PEG(2)

1.1 The effect of pH

PEG only has a weak affinity to SiO_2 and under standard conditions (pH 7.4) it has been shown that PEG-SLB formation by liposome fusion above the mushroom-to-brush transition is prevented[1]. Addition of 20 mM EDTA to the TBS buffer allows the formation of PEG-SLBs with DOPE-PEG(2) concentrations up to 10 mol% which is far in the brush regime. The resulting enhanced PEG-SLB formation could originate from interactions of EDTA with PEG or the SiO_2 surface, or from the lower pH of TBS + 20 mM EDTA (pH 5.0 ± 0.1) than of TBS (pH 7.4). TBS cannot be set to a pH as low as 5. Thus a control using acetate buffer suitable for low pH was chosen. It was prepared by mixing 0.1 M acetic acid (CH_3COOH; Sigma, Switzerland) with 0.1 M sodium acetate ($C_2H_3NaO_2$; Sigma, Switzerland) and 150 mM sodium chloride (NaCl) in water. For 1 liter of buffer, the solutions were diluted in the proportion of 357 ml of acetic acid with 643 ml sodium acetate to obtain buffer at pH 5. Fig. 1 (a) shows QCM-D curves of 10 mol% DOPE-PEG(2) in TBS + 20 mM EDTA (blue ▵) and in acetate buffer (red ○). PEG-SLBs formation proceeded in TBS + 20 mM EDTA (pH 5.0) as well as in acetate buffer (pH 5.0). This indicates that the essential attribute for PEG-SLB formation above the mushroom-to-brush transition is lowering the buffer pH. In TBS at a pH of 7.4 the QCM-D curve for 6 mol% DOPE-PEG(2) (black ▫) only shows low adsorption of intact liposomes as judged from the $-\Delta D/\Delta f$ ratio.

[a] *Laboratory for Surface Science and Technology, Department of Materials, ETH Zurich, Zurich, Switzerland*
[b] *Institut Pluridisciplinaire de Recherche sur l'Environnement et les Matériaux, Pau, France.*
[c] *Department of Nanobiotechnology, University of Natural Resources and Life Sciences Vienna, Vienna, Austria. E-mail: erik.reimhult@boku.ac.at*

Fig. 1 (b) shows the adsorption of 0.1 mg/ml methoxy PEG(5k) (mPEG(5)) on SiO_2 in TBS (black ▫), TBS + 20 mM EDTA (blue ▵) and acetate buffer (red ○). Experiments were performed under constant flow of 20 µl/min and the arrows indicate the injection of mPEG in the QCM-D cell. Changes of Δf and ΔD before the mPEG injection are due to the change to different buffer solution after obtaining the baseline in ultrapure water.

The QCM-D measurements show a higher affinity of mPEG at a lower pH value evidenced by $|\Delta f| \approx 1.5$ - 2 Hz for TBS + EDTA and acetate buffer while for TBS $|\Delta f| < 0.3$ Hz. The mechanism behind enhanced PEG-SLB formation at lower pH therefore is tentatively explained by a lower surface density of hydroxyl groups on the SiO_2 surface at pH 5.0 compared to pH 7.4. Weaker silica-water interaction correlates with increased adsorption of PEG from solution[2,3], which results in a decisive increase of the concentration of adsorbed liposomes at the surface triggering the PEG-SLB formation process[4]. It can be concluded that at pH 5.0 the PEG-SLB formation is facilitated on SiO_2 surfaces, which at least in part is due to the increased affinity of the PEG shell of the liposomes to the SiO_2 surface.

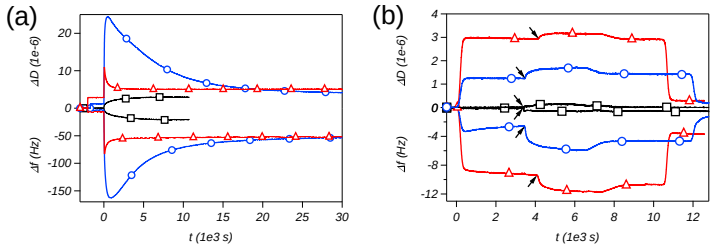

Fig. 1 QCM-D measurements of PEG-SLB formation kinetics and methoxy PEG adsorption on SiO_2. (a): 10 mol% DOPE-PEG(2) in TBS + 20mM EDTA (blue ○), 10 mol% DOPE-PEG(2) in acetate buffer (red △) and 6 mol% DOPE-PEG(2) in TBS (black ▫). (b): 0.1 mg/ml mPEG(5) in TBS+20mM EDTA (blue ○), in acetate buffer (red △) and in TBS (black ▫).

1.2 Estimation of the intact vesicle percentage in the 10 mol% PEG-SLB from QCM-D data

To exclude that intact vesicles in the PEG-SLB cause the complete slow-down of the lipid mobility we estimate a vesicle coverage in the 10 mol% PEG-SLB from the QCM-D data. The PEG-SLB with 6 mol% is used as a reference since it is confirmed by QCM-D and FRAP to be a low-defect SLB with high lipid mobility. In a linear approximation the QCM-D data of the 10 mol% PEG-SLB is composed of a SLB contribution (f_{SLB}, D_{SLB}) and a vesicle contribution ($f_{vesicle}$, $D_{vesicle}$). The final QCM-D signal is the sum, i.e. $\Delta f = f_{SLB} \cdot x + f_{vesicles} \cdot y$, with x, y the respective fractions of the two contributions and $x + y = 1$.

From this linear extrapolation a total vesicle coverage of 2.4 - 4.2 % is estimated.

$$f_{\text{vesicle}} = -164\ \text{Hz}$$
$$\Delta f_{6\ \text{mol\%}} = -44.7\ \text{Hz}$$
$$\Delta f_{10\ \text{mol\%}} = -49.7\ \text{Hz}$$

$$1 = x + y$$
$$\Delta f_{10\ \text{mol\%}} = \Delta f_{6\ \text{mol\%}} \cdot x + f_{\text{vesicle}} \cdot y$$
$$x = 95.8\%$$
$$y = 4.2\%$$

$$D_{\text{vesicle}} = 23 \cdot 10^{-6}$$
$$\Delta D_{6\ \text{mol\%}} = 2.2 \cdot 10^{-6}$$
$$\Delta D_{10\ \text{mol\%}} = 2.7 \cdot 10^{-6}$$

$$1 = x + y$$
$$\Delta D_{10\ \text{mol\%}} = \Delta D_{6\ \text{mol\%}} \cdot x + D_{\text{vesicle}} \cdot y$$
$$x = 97.6\%$$
$$y = 2.4\%$$

1.3 Local density variations as observed in FRAP measurements for 10 mol% DOPE-PEG(2)

Fig. 2 shows a FRAP series of a 10 mol% DOPE-PEG(2) SLB with 1 mol% NBD-PC (main lipid component label). The fluorescence intensity of the bleached spot does not recover, but locally frayed edges are visible indicating local density variations and some limited mobility in confined regions (see arrow in Fig. 2). Such local density variations could be responsible for the two populations found in force-distance measurements of 8 and 10 mol% DOPE-PEG(2) SLB samples.

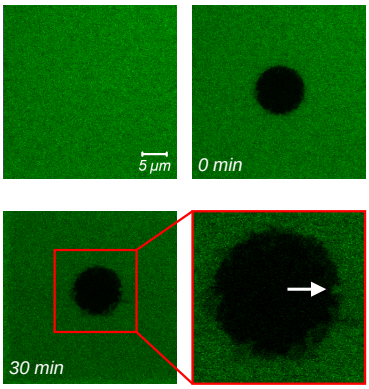

Fig. 2 FRAP series of 10 mol% DOPE-PEG(2) SLB where the main lipid component was labelled. The arrow is indicating a local denisty variation with local, partial fluorescence recovery.

2 Additional remarks on the derivation of the force profile for mobile polymer tethers

Recapitulation of the equations from the main text:

Radius of gyration:	$R_g = a\left(\frac{n}{6}\right)^{1/2}$
Flory radius:	$R_F \approx an^{3/5}$
Mushroom regime:	$s > R_F^2$
Brush regime:	$s < R_F^2$

It is a the monomer length, n the number of monomers, A the average area per lipid molecule, m the mole fraction of polymer lipids and $s = \frac{A}{m}$ the surface area per chain.
The interaction free energy per chain in the mushroom regime is determined by conformational entropy losses upon confinement of individual swollen coils and is given by[5]

$$E_{\text{mushroom}}(H,s) \approx k_B T \kappa \left(\frac{R_g}{H}\right)^{5/3} \tag{1}$$

where κ is a numerical coefficient of the order of unity (set as unity in the following), where H is the height of the compressing tip above the surface (with curvature radius much larger than the coil size), k_B is the Boltzmann constant and T the temperature.

The free energy per chain in the compressed brush regime can be calculated using the strong stretching self-consistent field approximation[6,7] and is given by[8,9]

$$E_{\text{brush}}(H,s) = \frac{5}{9}E_0\left[\left(\frac{H}{H_0}\right)^2 - \frac{1}{5}\left(\frac{H}{H_0}\right)^5 + \frac{H_0}{H}\right] \tag{2}$$

with E_0 the free energy of the free (uncompressed) brush

$$E_0(s) = k_B T \frac{9\pi^{2/3}}{10} n (v/a^3)^{2/3} (s/a^2)^{-2/3}. \tag{3}$$

The equilibrium height of the uncompressed brush, H_0, is found from the condition

$$\left(\frac{\partial E(H,s)}{\partial H}\right)_s = 0$$

and is given by

$$H_0(s) = \left(\frac{8}{\pi^2}\right)^{1/3} na (v/a^3)^{1/3} (s/a^2)^{-1/3} \tag{4}$$

The excluded volume parameter of a monomer unit v is given by $v \sim a^3$.

The force per unit area arising upon compression of the brush at $H \leq H_0$ can be found as

$$f(H,s) = -\frac{1}{s}\left(\frac{\partial E_{\text{mushroom/brush}}(H,s)}{\partial H}\right)_s \tag{5}$$

Substituting the energy from the mushroom $E_{\text{mushroom}}(H,s)$ and brush regime $E_{\text{brush}}(H,s)$, the force (per unit area) is given by

$$f(H,s)_{\text{mushroom}} = \frac{5}{3}\frac{k_BT\kappa}{sH}\left(\frac{R_g}{H}\right)^{5/3} \tag{6}$$

$$f(H,s)_{\text{brush}} = -\frac{5}{9}\frac{E_0(s)}{sH_0(s)}[2(H/H_0(s)) - (H/H_0(s))^4 - (H_0(s)/H)^2] \tag{7}$$

And as given in the main text, the chemical potential of a chain in the free mushroom or brush with given surface area s is found as

$$\mu_0(s) = \begin{cases} -k_BT\ln(s/a^2) & s > R_F^2 \\ E_0(s) - s\frac{\partial}{\partial s}E_0(s) - k_BT\ln(s/a^2) & s < R_F^2 \end{cases} \tag{8}$$

and the chemical potential in the compressed area in the mushroom ($s > R_F^2$) and brush regime ($s < R_F^2$) respectively is given by

$$\mu(H,s) = \begin{cases} E_{\text{mushroom}}(H,s) - s\left(\frac{\partial}{\partial s}E_{\text{mushroom}}(H,s)\right)_H - k_BT\ln(s/a^2) & s > R_F^2 \\ E_{\text{brush}}(H,s) - s\left(\frac{\partial}{\partial s}E_{\text{brush}}(H,s)\right)_H - k_BT\ln(s/a^2) & s < R_F^2 \end{cases} \tag{9}$$

3 PEG-lipid distribution

3.1 Cryo-transmission electron microscopy

250 nm core diameter SiO_2 nanoparticles (G. Kisker, Germany) were dispersed at 10 mg/ml in Millipore water and sonicated for 1 h. These nanoparticles were added to a TBS based suspension of 1 mg/ml POPC liposomes containing 6 mol% DOPE-PEG(2), where 20 mM EDTA was added. After fusing the liposomes on SiO_2 nanoparticles over night at room temperature, 3.5 µl drops of the suspension were dried for 1 min on holey carbon film TEM grids (300 mesh Cu grids, R3.5/1 Quantifoil) which had previously been glow discharged for 30 s (Emitech K100X, Quorum Technologies). Samples were frozen by plunge freezing in liquid ethane using a Vitrorobot (FEI). The fast cooling rates achieved by plunge freezing allow for vitrifying water. Transmission electron micrographs were taken on a Philips CM12 microscope operated at 100 kV at liquid N_2 temperatures.

Fig. 3 (a) shows a PEG-SLB with 6 mol% DOPE-PEG(2) formed on a SiO_2 particle. The image on top shows a magnification of the section indicated by the arrow. The distance between the SLB (the region of the phosphate head groups can be identified from the dark border) and the particle surface suggests that only a space of a couple of nanometer exists to accomodate a thin layer of PEG in between. Fig. 3 (b) shows a

PEG-SLB with 1 mol% DOPE-PEG(5) on SiO_2 particles. The distance between the SLB and the particle surface again does not show a significant decoupling of the SLB from the surface. The particle in the case of 1 mol% DOPE-PEG(5) however seems to be shielded from surrounding liposomes by a layer, depicted as a brighter ring surrounding the particle and highlighted with an arrow. It is suggested that this layer is an exclusion zone created by the PEG of the outer leaflet of the PEG-SLB. The indications of an asymmetric distribution of the PEG-lipids in the PEG-SLB motivated the discussion in the article where two extreme scenarios for the PEG-lipid distribution between the leaflets were treated, namely (a) completely homogeneous and (b) only in the outer leaflet.

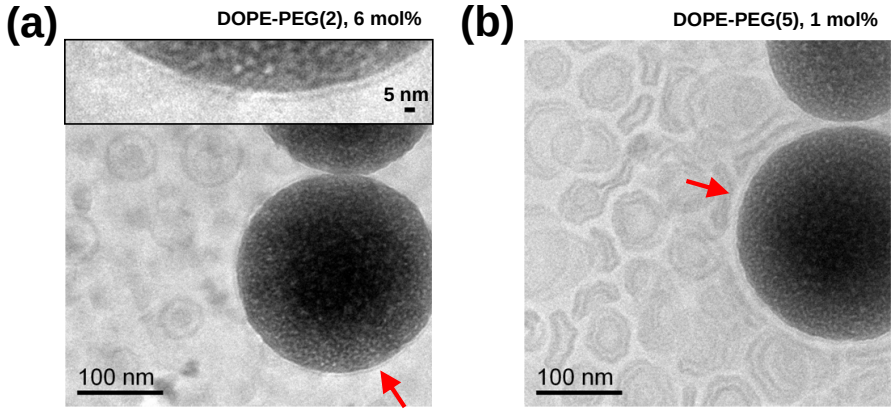

Fig. 3 Cryo-TEM measurement of PEG-SLBs formed on 250 nm SiO_2 particles with (a): 6 mol% DOPE-PEG(2) and (b): 1 mol% DOPE-PEG(5).

3.2 Force-distance measurements

Force-distance measurements on PEG-SLBs formed on planar substrates nonetheless indicate a thickness of PEG-SLBs which corresponds to two PEG-layers. Fig. 4 presents onset data of the force-distance curves from measurements with DOPE-PEG(2) in a POPC matrix with concentrations of 0, 2, 4, 6, 8 and 10 mol% DOPE-PEG(2) where the thickness of a POPC SLB, i.e. 4.7 nm[10,11] was subtracted. The onset of the compression force is determined by reading out the distance when a defined set point in the force value is crossed. The force set points are chosen in the range of 10 - 40 pN and the force-distance curves were smoothened by box smoothing. The onset values hence determine the first contact of the AFM tip with the polymer layer. Empty symbols in Fig. 4 are results from measurements with PLL-*g*-PEG modified AFM tips and filled symbols measurements with unmodified AFM tips. The red and blue curves in Fig. 4 compares the onset data with $R_F = an^{3/5}$ in the mushroom and $H_0(s) = \left(\frac{8}{\pi^2}\right)^{1/3} na \left(\frac{s}{a^2}\right)^{-1/3}$ in the brush regime[9] for one (red) and two

(blue) layers of PEG. The variables describe the number of monomers, n, the monomer length, a and the surface area per PEG chain, s.

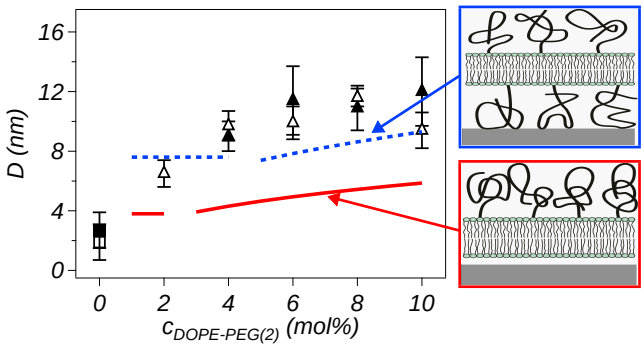

Fig. 4 Graphical representation of the onset forces of DOPE-PEG(2) with subtracted POPC thickness. Empty symbols are measurements with PLL-*g*-PEG modified AFM tips and filled symbols with unmodified AFM tips. The symbols identify POPC (▫) and DOPE-PEG(2) (△). The blue, dashed line represent the PEG thickness expected for homogeneous PEG-lipid distribution and the red, solid line for PEG-lipids present in one leaflet only.

The onset values are generally slightly larger than the expected thickness values for an arrangement with PEG-lipids distributed in both leaflets and significantly larger than expected values for PEG-lipids located only in one leaflet. The measurements therefore support an arrangement with considerable presence of PEG-lipids in both SLB leaflets in agreement with our previous work[1].

3.3 Mobility

An asymmetric distribution of PEG-lipids should result in a lower or vanishing concentration of PEG-lipids in the lower leaflet. In the main text of this article, it was shown that PEG-lipid concentrations slightly below 10 mol% effectively hinder the motion of matrix POPC lipids. In an asymmetric distribution of PEG-lipids the decreased concentration of PEG-lipids in the lower leaflet should not hinder the motion of POPC lipids and should result in two mobile fractions with significantly different diffusion coefficients or one mobile and one immobile fraction of NBD-PC labeled lipids. It has been shown that lipid monolayers on alkyl self-assembled monolayers are mobile,[12] which demonstrates that the tail-tail interactions with an immobile upper leaflet should not constrain lipid mobility and POPC lipids are known to be mobile in both leaflets in SLBs formed on SiO_2[13]. Two mobile fractions or one mobile and one immobile fraction of NBD-PC labeled lipids were however never observed in FRAP measurements despite our use of a FRAP method able to discern multiple mobile fractions[14]. Therefore the FRAP measurements further support an arrangement with a reasonably equal distribution of PEG-lipids between the two leaflets.

3.4 Discussion of the PEG-lipid distribution

The distribution of PEG-lipids in SLBs is influenced by several factors such as the geometry of the support (i.e. curvature), the chemical composition and thermodynamic fluctuations.

In cryo-TEM measurements on 250 nm SiO_2 particles the supporting substrate has a significantly larger curvature compared than a flat substrate. For a curved membrane the PEG-lipid distribution is not necessarily symmetric and the results may not be directly transferable to planar SLBs. Additionally, for cryo-TEM of PEG-SLBs on nanoparticles, the resolution of approximately 2 nm[15] and determination of the correct focal plane are major complications for correct interpretation of the thickness of the depletion layer and membrane spacing to the substrate.

Further, the distribution of PEG-lipids in SLBs on flat substrates may be significantly influenced by the chemical state of the surface determining its Hamaker constant, and hence on the cleaning procedure, the buffer conditions and composition of the used silica glass.

Force-distance measurements with an AFM and thickness estimations are always based on assumptions of a monomer density profile, although the by us chosen profile has been shown to describe polymer configurations reasonably well[16]. Undulations of SLBs on the order of a few nanometers can further result in increased interaction distances measured by AFM.

Concluding, the presented data set, in our opinion, demonstrates support for a reasonably equal distribution of PEG-lipids between the two leaflets in planar SLBs.

4 Force-distance measurements with poly(L-lysine)-*graft*--poly(ethylene glycol) modified AFM tips

Control measurements with poly(L-lysine)-*graft*-poly(ethylene glycol) (PLL-*g*-PEG) coated AFM tips in Fig. 5 show the same behavior as uncoated silicon AFM tips presented in the article in Figure 4. AFM tips were surface modified by immersing the cleaned cantilevers in a 1 mg/ml filtered solution of PLL(20 kDa)-*g*[3.5]-PEG(2 kDa) (SuSoS AG, Switzerland) in 10 mM Hepes (pH 7.4) for 30 min, followed by rinsing with ultrapure water and subsequent drying with a gentle stream of nitrogen as reported by Pasche *et al.*[17]. It proves that PLL-g-PEG can be used to passivate the AFM tip to prevent adsorption of liposomes since it forms a dense PEG brush on the tip and that no significant differences on the interaction distance and forces were found between modified and unmodified AFM tips for DOPE-PEG(2) compression and rupture.

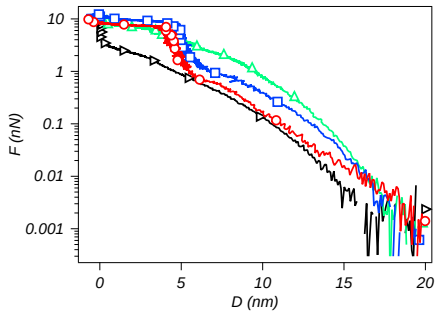

Fig. 5 Force-distance measurements with a PLL-*g*-PEG modified AFM tip. 4 mol% (red ◦, 264 force-curves), 6 mol% (blue ▫, 250 force-curves) and 8 mol% (green ▵, 175 force-curves) and 10 mol% (black ▹, 346 force-curves) DOPE-PEG(2) systems.

References

[1] S. Kaufmann, G. Papastavrou, K. Kumar, M. Textor and E. Reimhult, *Soft Matter*, 2009, **5**, 2804 – 2814.

[2] J. Rubio and J. A. Kitchener, *Journal of Colloid and Interface Science*, 1976, **57**, 132–142.

[3] A. Kanta, R. Sedev and J. Ralston, *Langmuir*, 2005, **21**, 2400–2407.

[4] P. S. Cremer and S. G. Boxer, *Journal Of Physical Chemistry B*, 1999, **103**, 2554–2559.

[5] P. G. de Gennes, *Scaling Concepts in Polymer Physics*, Cornell University Press, 1979.

[6] A. Skvortsov, I. Pavlushkov, A. Gorbunov, Y. Zhulina, O. Borisov and V. Pryamitsyn, *Polymer Science U.S.S.R.*, 1988, **30**, 1706–1715.

[7] S. T. Milner, T. A. Witten and M. E. Cates, *Europhysics Letters*, 1988, **5**, 413–418.

[8] S. T. Milner, T. A. Witten and M. E. Cates, *Macromolecules*, 1988, **21**, 2610–2619.

[9] E. B. Zhulina, O. V. Borisov and V. A. Priamitsyn, *Journal Of Colloid And Interface Science*, 1990, **137**, 495–511.

[10] S. J. Johnson, T. M. Bayerl, D. C. McDermott, G. W. Adam, A. R. Rennie, R. K. Thomas and E. Sackmann, *Biophysical Journal*, 1991, **59**, 289–294.

[11] J. F. Nagle and S. Tristram-Nagle, *BBA - Biomembranes*, 2000, **1469**, 159–195.

[12] V. von Tscharner and H. M. McConnell, *Biophysical Journal*, 1981, **36**, 421–427.

[13] L. Zhang and S. Granick, *J. Chem. Phys.*, 2005, **123**, 211104–4.

[14] P. Jönsson, M. P. Jonsson, J. O. Tegenfeldt and F. Höök, *Biophysical Journal*, 2008, **95**, 5334–5348.

[15] S. Mornet, O. Lambert, E. Duguet and A. Brisson, *Nano Letters*, 2005, **5**, 281–285.

[16] A. K. Kenworthy, K. Hristova, D. Needham and T. J. Mcintosh, *Biophysical Journal*, 1995, **68**, 1921–1936.

[17] S. Pasche, M. Textor, L. Meagher, N. D. Spencer and H. J. Griesser, *Langmuir*, 2005, **21**, 6508–6520.